Heliyon 5 (2019) e01946

Contents lists available at ScienceDirect

Heliyon

journal homepage: www.heliyon.com

Heliyon

Synthesis and characterization of tetra-ganciclovir cobalt (II) phthalocyanine for electroanalytical applications of AA/DA/UA

Mounesh [a], Pari Malathesh [a], N.Y. Praveen Kumara [a], Bhvimane Sanna Jilani [a], C.D. Mruthyunjayachari [b], K.R. Venugopala Reddy [a,*]

[a] Department of Chemistry, Vijayanagara Shrikrishnadevaraya University, Ballari, 583 105, Karnataka, India
[b] Department of Industrial Chemistry, Sahyadri Science College, Shivamogga, 577 203, Karnataka, India

ARTICLE INFO

Keywords:
Analytical chemistry
Electrochemistry
CoTGPc
Amperometry sensors
Ascorbic acid
Dopamine
Uric acid

ABSTRACT

Cobalt (II) phthalocyanine embedded with ganciclovir units has been synthesized by a novel method using tetracarboxylic phthalocyanine reported for the first time. The synthesized dark green colored complexes were characterized by electronic spectroscopy, elemental analysis, FT-IR, MASS and XRD. Thermal stability study reveals that the newly synthesized complex was stable up to 300 °C and XRD patterns showed amorphous nature of the complex. In the present work, the synthesized complex was characterized by cyclic voltammetry and shows the redox behavior corresponding to central metal (Co^{+II}/Co^{+I}) of the complex. Three biomolecules are well-separated by their oxidation peaks in simultaneous determination predicting the potentials for (-128, 335, and 723 mV) with highly increasing current. The low detection limit of AA, DA, and UA were 0.33, 0.03 and 0.10 μmol by CV method and good responses of amperometric and DPV technique. The modified tetra substituted CoTGPc/GCE exhibit an excellent electrocatalytic activity, stability, high sensitivity, good linearity, and selectivity without losing its catalytic activity and proves to be a versatile chemical sensor for commercial pharmaceutical samples, vitamin C tablets, and dopamine injections.

1. Introduction

Ascorbic acid (AA) is popularly known for its antioxidant properties and often present in the human diet as a vital vitamin. It also has an excellent curative effect for the common cold, mental illness, and barrenness [1, 2] It influences essential physiological processes, such as cell division, gene expression and activation of biological defense mechanisms [3]. Dopamine (DA) is an excitatory neurotransmitter that plays an important role in the physiological events such as the central nervous, cardiovascular, renal and hormonal systems [4]. Low levels of DA may cause neurological disorders, such as Parkinson's disease and schizophrenia [2, 5], considering the importance given to the determination of DA concentrations [6, 7, 8]. Uric acid (UA) is the primary end product of purine metabolism. The abnormal concentration will lead to many diseases, including hyperuricemia, gout, and leukemia [9, 10]. In summary, AA, DA, and UA are very important small molecules, and they are usually coexisting together in real biological samples. Therefore, constructing a high sensitivity and well selectivity sensor for their simultaneous determination is highly desirable for analytical application and diagnostic research. Macromolecules and N4-macrocycles are versatile materials in surface modification of the electrodes because of their extended conjugation, chemical, and thermal stability and excellent catalytic activities. Phthalocyanines (Pcs) are the N4-macrocyclic molecules having similarities in life-sustaining biomolecules like heme-protein and chlorophyll and shows redox behavior due to the presence of delocalization of π-electrons and the interaction of the central metal atom with the Pc N4-macrocycle. Metal phthalocyanines are organic macrocyclic molecular catalysts with metal atoms at the center and possess rich redox chemistry [11, 12]. The central metal ion of phthalocyanines can reversibly bind with reactants and hence they exhibited good electrocatalytic activity to many important reactions. Cobalt phthalocyanine and its derivatives (CoPCs) are the most widely studied phthalocyanines as mediator/electrode modifiers attributed to their widespread electrochemical applications [13]. These PCs play an excellent role in developing sensors because of their biocompatibility, chemical inertness, and good catalytic activity. Further, Pc moieties have

* Corresponding author.
E-mail address: venurashmi30@gmail.com (K.R. Venugopala Reddy).

https://doi.org/10.1016/j.heliyon.2019.e01946
Received 21 February 2019; Received in revised form 4 May 2019; Accepted 7 June 2019

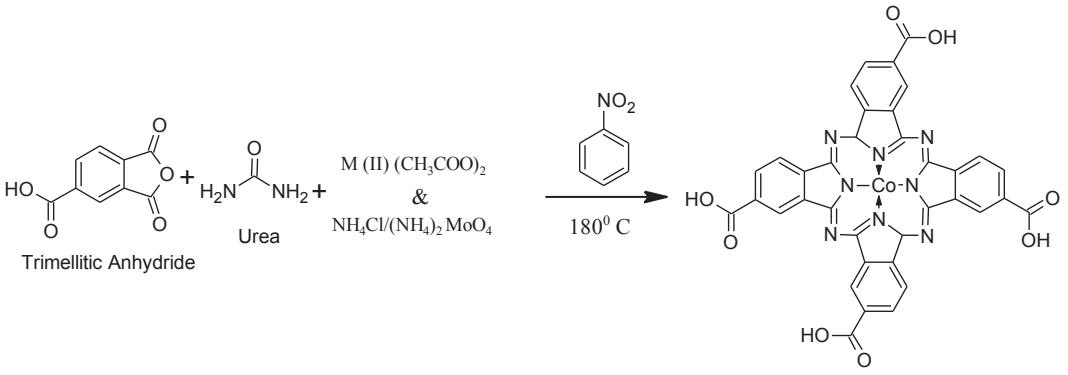

Scheme 1. Synthesis of tetra-carboxylic acid cobalt (II) phthalocyanine (CoTCPc).

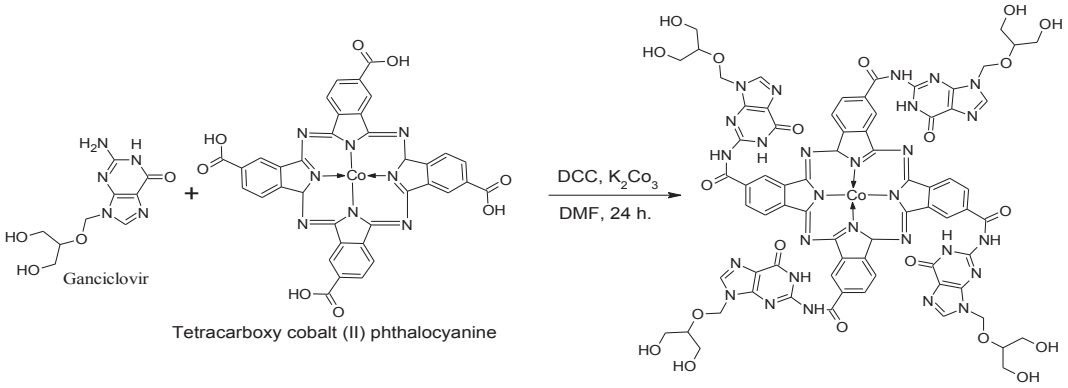

Scheme 2. Synthesis of tetra-ganciclovir cobalt (II) phthalocyanine (CoTGPc).

Table 1
Elemental analysis of tetra ganciclovir cobalt (II) phthalocyanine.

Complex (Yield) colour	Empirical formulae (formula) weight	Elemental analysis (%) Found (calcd)
tetra-ganciclovir cobalt (II) phthalocyanine (91%) Dark green	$C_{72}H_{62}CoN_{28}O_{20}$ (1698.3625)	C; 50.86: (50.43) H; 3.82: (3.48) N; 23.08: (22.91) Co; 3.46: (3.36)

16 vacant sites at the periphery of the four isoindole units and that can be substituted with a variety of functional groups for tailoring the properties. This present work: The ganciclovir embedded cobalt (II) phthalocyanine is used to modify the GCE, for the determination of simultaneous and individual analytes for the detection of DA, AA, and UA, the modified CoTGPc/GC electrode is a good electrocatalyst and indicates the high sensitivity, stability, good repeatability and reproducibility.

2. Experimental

2.1. Precursors

Ganciclovir and Uric acid, N, N'Dicyclohexylcarbodiimide were purchased from Sigma Aldrich. N, N′ Dimethylformamide of D-tedia (USA), Potassium carbonate anhydrous was purchased from Merck Co. DA, AA, UA, methanol and pH = 7 phosphate buffer solution (PBS) was purchased from Hi-Media Laboratories Pvt. Ltd. (INDIA).

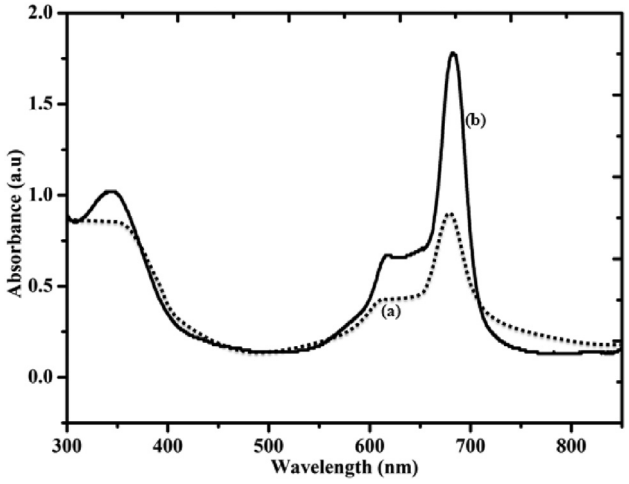

Fig. 1. UV-Vis spectra of (a) tetra ganciclovir cobalt (II) phthalocyanine and (b) tetra carboxy cobalt (II) Phthalocyanine.

2.2. Synthesis

2.2.1. Synthesis cobalt tetracarboxylic phthalocyanine (CoTCPc)

CoTCPc was synthesized by a slight modification of the procedure reported in the literature [14, 15, 16]. The finely grounded mixture of trimellitic anhydride (0.4 mmol), urea (0.1mol), the catalytic quantity of

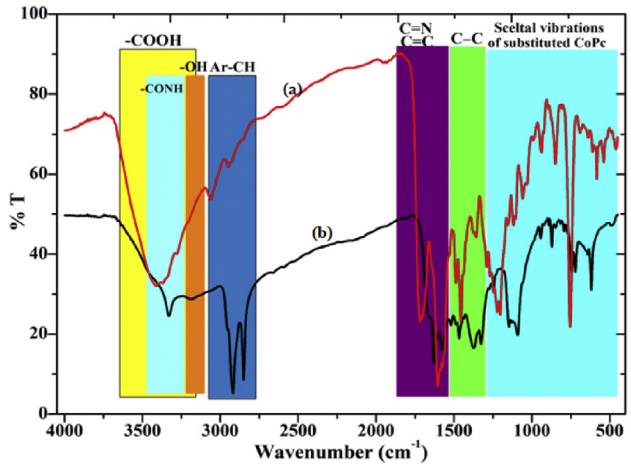

Fig. 2. FTIR spectra of (a) tetra ganciclovir cobalt (II) Phthalocyanine and (b) tetra carboxy cobalt (II) Phthalocyanine.

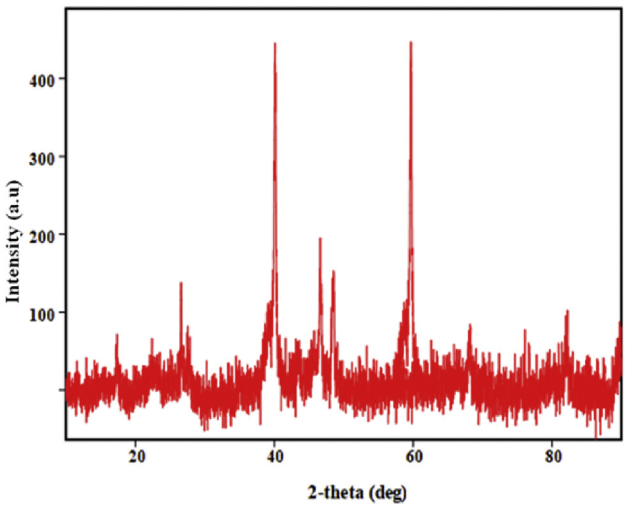

Fig. 4. XRD spectra of tetra ganciclovir cobalt (II) Phthalocyanine.

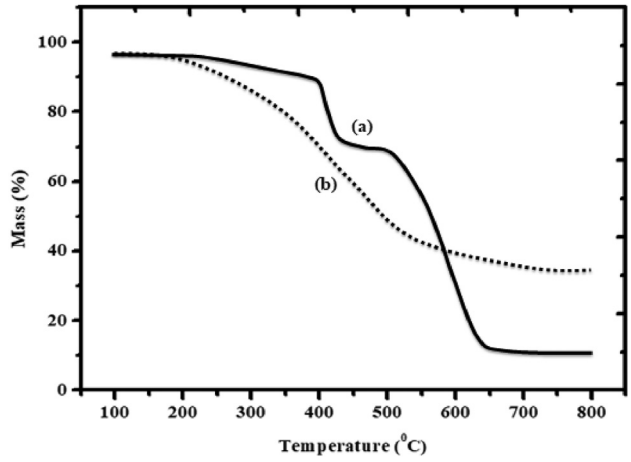

Fig. 3. TGA analysis of (a) tetra ganciclovir cobalt (II) Phthalocyanine and (b) tetra carboxy cobalt (II) Phthalocyanine.

ammonium molybdate (0.4 mmol) and Co $(CH_3COO)_2$ (0.1 mmol) was charged into 25 mL of DMSO and refluxed for 4 h at 180 ± 5 °C (Scheme 1). The dark green colored complex was washed with alcohol and followed by 0.5 mol L^{-1} of HCl, 0.5 mol L^{-1} NaOH in combination with saturated NaCl solutions. Finally, the crude product was thoroughly washed with distilled water until free from acid and dried over P_2O_5 in a vacuum desiccator.

2.2.2. Synthesis of cobalt (II) tetra ganciclovir phthalocyanine (CoTGPc)

CoTGPc was synthesized by modifying the available procedure reported in literature [2, 17, 18, 19] CoTCAPc (0.073 g, 0.0098 mmol), K_2CO_3 (0.68 g, 0.0098 mmol) was placed in a clean and dry 250mL round bottomed (RB) flask and dissolved in dimethylformamide (DMF, 20 ML) along with catalytic quantity of N, N' Dicyclohexylcarbodiimide (DCC). The RB flask was constantly stirred for 20 min. Ganciclovir solution (0.1 g, 0.0392 mmol) was added followed by constant stirring (Scheme 2). A dark green precipitate has appeared after 48 h and the reaction mixture was allowed to cool and poured into ice cold water and purified with successive hot and cold water followed by hexane.

The product was dried over P_2O_5 in a vacuum desiccator. Yield: 80%. Anal. CoTGPc, Mol.wt. 1698.36. $C_{72}H_{62}CoN_{28}O_{20}$: Calc. (%) C, 50.86; H, 3.82; N, 23.08; Co, 3.46. Found: C, 50.42; H, 3.76; N, 22.91; Co, 3.36. Absorption spectra, λmax (nm): 340, 615, 685. FTIR, (Cm^{-1}): 619, 718, 749, 840, 871, 954, 1091, 1144, 1243, 1327, 1373, 1442, 1547, 1632, 2888, 3177 and 3329.

2.3. Preparation of modified electrodes

Prior to modification, the GCE surface was polished to the mirror surface with 0.5 mm alumina slurries using a polishing pad and rinsed thoroughly with double distilled water, sonicated 5 min in acetone and 5 min in water, and dried in air. The ultrasonication for 20 min was to disperse 5 mg of CoTGPc in dry DMF solvent and finally, the GCE was coated with 5 μL CoTGPc suspension and dried at room temperature in the air-drier. This electrode was used for voltammetric detection of DA, AA, and UA independently and simultaneously.

2.4. Characterization methods

Absorption spectra of 0.01mM CoTGPc in DMSO have been performed in the range of 200–800 nm at room temperature on a Shimadzu UV-550 spectrophotometer using a 1 cm path length cuvette. FTIR spectra were recorded as KBr pellet in the region of 4000-500 cm^{-1} using Perkin Elmer Spectrum 100 FT-IR Spectrometer. XRD was performed using a Bruker Advanced D8 diffractometer Cu-Ka-radiation source. Mass spectra the final compound was taken by ESI-MS MALDI-Micromass Q-TOF2 equipment. Thermogravimetric analysis was performed on a Mettler Toledo instrument with a heating rate of 20 °C/min and a nitrogen flow rate of 50 mL/min.

All the electrochemical measurements were carried out on a CHI620E electrochemical workstation, USA, with a conventional three-electrode system. The composition of internal solution is 3.0 M KCl electrolyte solution in Ag/AgCl reference electrode, GCE as working electrode and platinum wire as a counter electrode. The sensing studies of DA, AA, and UA using modified GCE (individually and simultaneously) were carried out using 0.1 M of (pH = 7) phosphate buffer electrolyte in a nitrogen atmosphere.

3. Results and discussion

The schematic for the synthesis of CoTGPc complex is shown in Scheme 2. The amine group of the ligand is reacted with a carboxylic group of CoTCPc to yield amide bridged CoTGPc. The elemental analysis data fairly agreed with the theoretical values indicating the synthesized complexes are pure in nature (Table 1). The synthesized complex has been characterized by various spectroscopic as well as electrochemical techniques.

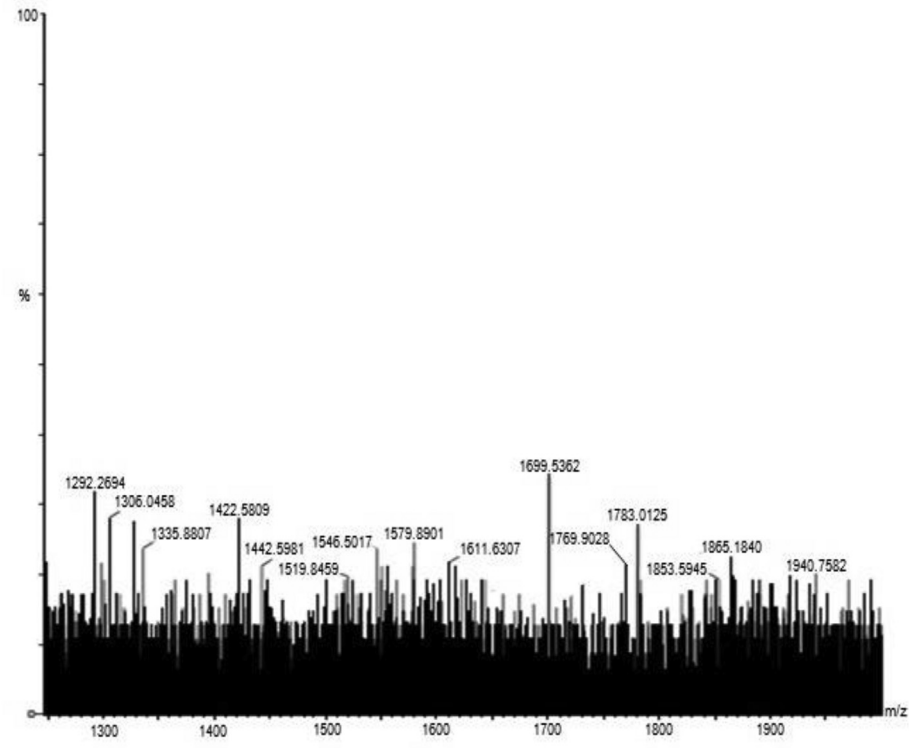

Fig. 5. ESI-MS mass spectrum of tetra ganciclovir cobalt (II) phthalocyanine.

Table 2
Analytical characteristics determination of AA, DA and UA by the tetra ganciclovir cobalt (II) phthalocyanine/GCE.

Electrodes	Methods	[a] A	[b] E_p (mV)	[c] DOL (μmol)	Linear regression (Y)	(R^2)	Linear range	[d] Sen (μA μM^{-1})	Ref.
PtAu hybrid film modified electrode	CV	AA	190	-	-	-	0.103–0.165mM	0.008	[25]
		DA	350	-	-	-	0.024–0.384mM	0.05	
		UA	520	-	-	-	0.02–0.336mM	0.015	
[Ni(phen)$_2$]2+/SWCNTs/GCE	CV	AA	130	-	-	-	30.0–1547 μM	-	[38]
		DA	334	-	-	-	1–780 μM	-	
		UA	486	-	-	-	1–1407 μM	-	
CoTGPc/GCE	**CV**	**AA**	**-128**	**0.33**	**1.73 (AA)+3.47**	**0.999**	**2–10 μM**	**1.73**	**THIS WORK**
		DA	**245**	**0.03**	**2.54 (DA)+3.76**	**0.999**	**2–10 μM**	**2.54**	
		UA	**623**	**0.10**	**1.55(UA)+11.20**	**0.998**	**2–10 μM**	**1.55**	
	DPV	**AA**	**-131**	**0.50**	**2.88 (AA)+4.199**	**0.998**	**2–12 μM**	**2.88**	
		DA	**250**	**1.20**	**2.91 (DA)+4.20**	**0.999**	**2–12 μM**	**2.91**	
		UA	**610**	**0.50**	**2.99(UA)+4.26**	**0.999**	**2–12 μM**	**2.99**	
	CA	**AA**	**-200**[e]	**5.33**	**0.421 (AA)+1.746**	**0.995**	**5–45 μM**	**0.42**	
		DA	**400**	**6.50**	**0.831 (DA)+0.757**	**0.998**	**5–45 μM**	**0.83**	
		UA	**600**	**5.00**	**0.902(UA)+2.373**	**0.994**	**5–45 μM**	**0.90**	

[a] Analytes.
[b] Peak potential.
[c] Detection limit.
[d] Sensitivity.
[e] Applied potential.

3.1. UV-vis spectra

The synthesized CoTGPc in 0.01 mM solution DMSO were recorded in the range of 200–800nm (Fig. 1). Characteristic intense absorption Q band in the range of 600–720 nm, was attributed to the π→π* transitions from the highest occupied molecular orbital (HOMO) to the lowest unoccupied molecular orbital (LUMO) of the Pc ring. The Q-band absorptions within the range of 666–678 nm below 700 nm confirm that the central metal was in the complex in the form of cobalt (II). The absorption peaks in the range of 350–300 nm corresponds to B band, a shoulder peak in the range of 610–625 nm corresponds to the oligomer and dimmer of PCs and an intense peak within the UV range of were due to the transitions from the deeper π levels to the LUMO a shoulder peak at 680–700 nm for the Q-band [20, 21]. The absorption spectrum of CoTGPc (Fig. 1 inset a curve) showed a red shift compared to parental CoTCPc (Fig. 1 inset b curve) may be due to the extensive conjugation and the ganciclovir at the periphery of the Pc moiety. Hence, the absorption spectrum of this novel complex can be tuned for spectral shifts by varying the substituent attached to the ring of the Pc complex.

3.2. FT-IR studies

The FTIR spectra were recorded in the range of 500–4000 cm^{-1} for the synthesized complex of CoTGPc. A broad peak observed in the range

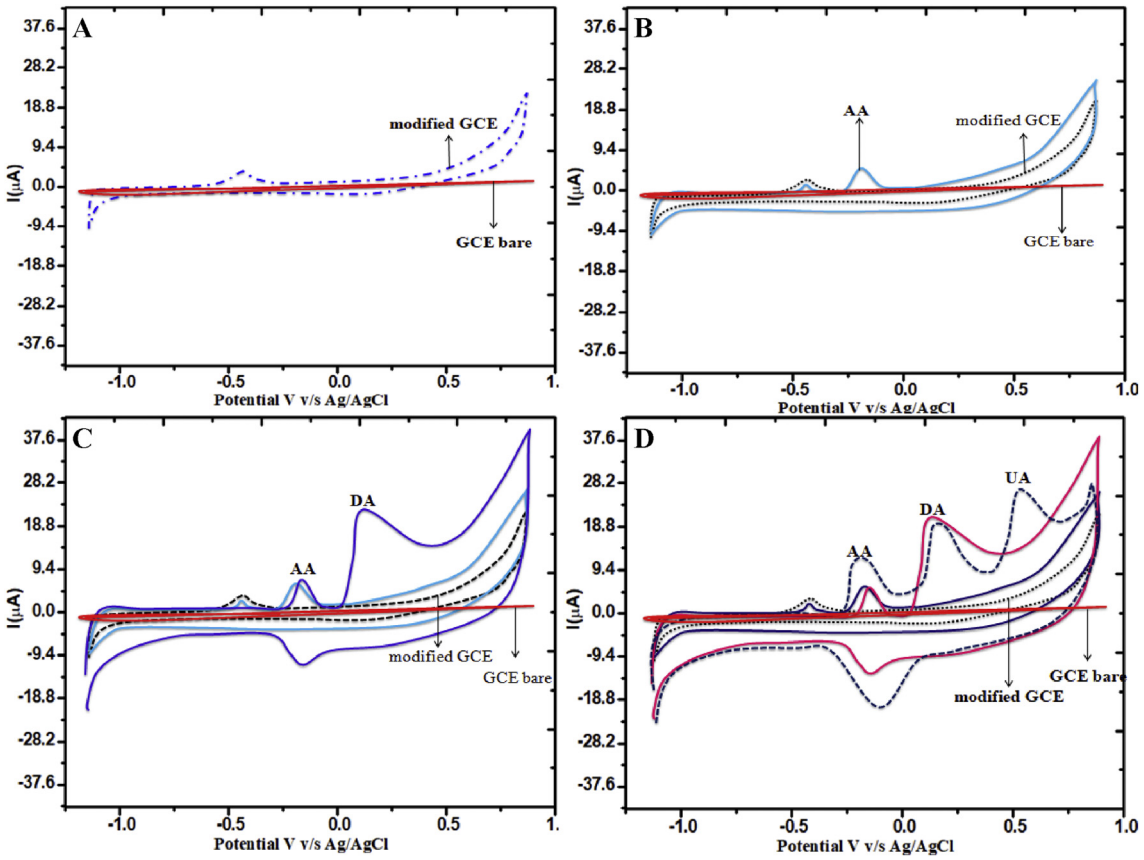

Fig. 6. CV plots of CoTGPc/GC electrode in PBS (pH=7) electrolyte system peaks at; (A) modified CoPc/GCE (B) 10 μM AA, (C) 15 μM DA and (D) 20 μM UA. Scan rate=100 mVs^{-1}.

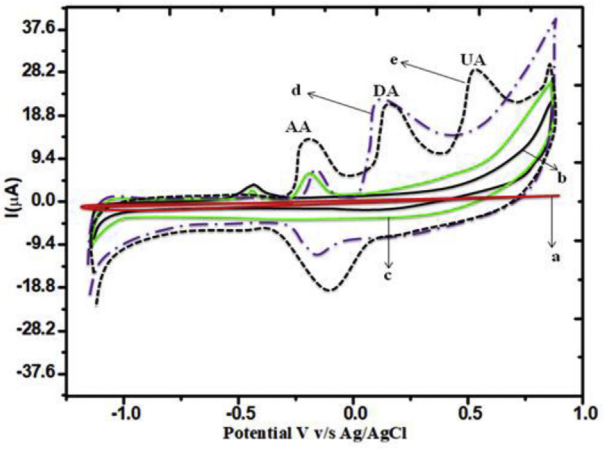

Fig. 7. CVs plot of CoTGPc/GCE electrode in PBS (pH=7) electrolyte system at peaks: inset (a) bare GCE, (b) CoTGPc/GCE, (c) 10 μM of AA, (d)15 μM of DA and (e) 20 μM of UA (black dots peak). Scan rate=50 mVs^{-1}.

3600-3200cm^{-1} for –COOH (Fig. 2 inset a curve) of CoTCPc disappears and a new peak at 3329 cm^{-1} was appeared and assigned to –CONH present in the complex (Fig. 2 inset b curve). An intense absorption peak at 3177 cm^{-1} (-OH), and the presence of a band in the region of 2919-2857 for (Ar-CH), the stretching vibrations of (C=N) and (C=C) group were observed near 1631–1632, and 1575-1518 and 1472, 1373, 1327, 1243, 1144, 1091, 954, 871,840, 749, 718, 619 these peaks are attributed to the various skeletal vibrations of substituted CoPc ring.

3.3. Thermogravimetric analysis

Fig. 3 inset b and a curve shows the thermogram of CoTCPc and CoTGPc. The CoTGPc was stable up to 425°C and CoTCPc was up to 300°C and the substitution of ganciclovir improves the thermal stability of CoTGPc (Fig. 3 inset a curve). The CoTGPc undergo three step degradation one at 425°C, second at 510°C and third at 630°C. 425°C corresponds to the loss of ganciclovir (49.5%), 510°C for loss of Pc ring (29.87%) and 630° C (20.62%) loss was in good agreement with CoO (Fig. 3 inset a curve). shows that the thermal stability of the tetra ganciclovir CoPc complex was higher than that of pure Pcs where the degradation temperature is significantly shifted to higher values(Fig. 3 inset b curve). [22].

3.4. Powder X-ray diffraction studies

Fig. 4 shows the Powder X-ray diffraction patterns (Fig. 4) for the synthesized complexes. The spectrum was recorded in the 2θ angle range of 0-100°. Highly noisy pattern and sharp peaks were observed at 2θ values 27.52°, 40.65°, 46.12°, 49.39°, and 60.05° indicates that CoTGPc was crystalline in nature. The d_{hkl} and 2θ values obtained were compared with the values reported in the literature (ICDD-PDF Files) and found to be in good agreement for the CoTGPc complex [23, 24].

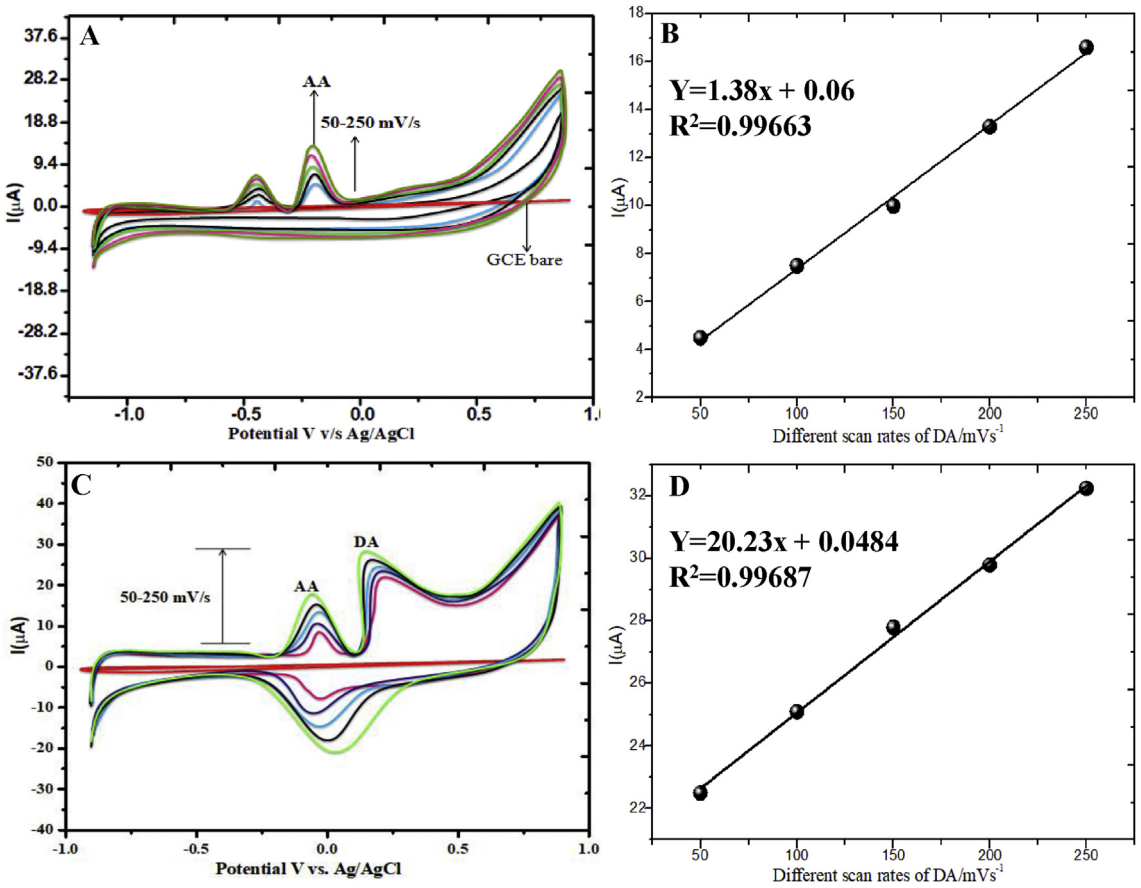

Fig. 8. CVs plot of CoTGPc/GCE in PBS (pH=7) electrolyte system peaks at; (A) Different scan rates of 10 μM AA, (B) Linear plot of positive peak current vs. different scan rates of AA/mV s^{-1}, (C) Different scan rate of 15 μM DA and (D) Linear plot of positive peak current vs. different scan rates of DA/mVs^{-1}.

3.5. Mass spectral studies

Fig. 5 shows the mass spectrum of CoTGPc with molecular mass 1699 against the calculated mass of 1698 which proves that the formation of the complex CoTGPc recorded in ESI-MALDI instrument.

3.6. Electrochemical studies

3.6.1. Simultaneous electrocatalytic oxidation of AA, DA, and UA

The electrocatalytic oxidation of AA, DA, and UA on the GCE was investigated by CV. The modified CoTGPc/GCE in PBS (pH = 7) electrolyte detects the cathodic peak potential -0.462 V without the target molecule Fig. 6A. The cathodic peak potential shift to lower potential -128 mV with a large shift of -334 mV in presence of target molecule AA, Fig. 6B. The addition of 15 μM of DA to the same system, shows anodic peak potential and high peak current (245 mV and 22.8 μA) Fig. 6C (Pink color line curve). To the same system addition of 20 μmol of UA predicts the oxidation at 623 mV and 27.91 μA Fig. 6D (dash line curve). The potential shift and current increase show the versatile electrocatalytic activity of CoTGPc/GCE and well-separated peaks for AA, DA, and UA in 20 μmol concentration. The results reflect that the use of CoTGPc/GCE, the addition of each of the interfering molecules there was well defined and regular shift of anodic peak potential [25, 26, 27, 28]. The electron mediating properties of CoTGPc/GCE towards the oxidation of AA, DA, and UA were detected by anodic peak potential. The modified GCE was the best CVs, DPV and CA techniques shows good oxidation responses for DA, AA, and UA. Therefore, the development of catalytic surfaces that can enhance and individualize the DA, AA, and UA has been a major subject of several pieces of research [29, 30, 31, 32]. The oxidation peak current of GCE was increased. Here, the oxidation of DA, AA, UA, or mixture mediated by oxidized form of GCE present in the solution. So this phenomenon of attributed to the mediated oxidation reaction state of GCE towards DA, AA, and UA respectively, as shown in Table 2.

3.6.1.1. Electrooxidation overlay plotting of AA, DA and UA. Experimental section of cyclic voltametry of tetra substituted ganciclovir cobalt (II) phthalocyanine/GC electrode as usual potential window (+0.8 to -1.2 V), predict the first unmodified GCE bare (Fig. 7 inset a curve). Modified GCE detecting the anodic peak potential and positive current (-452 mV, 6.42 μA) as shown in Fig. 7 inset b curve. 10 μM of AA to predict the anodic peak potential (-128 mV, 7.98 μA) Fig. 7 inset c curve. 15 μM of DA to detecting the positive peak potential and positive current (235 mV, and 22.8 μA) as shown in Fig. 7 inset d curve. And 20 μM of UA is predicting highly extensively positive peaks potential and positive current (623 mVs^{-1} and 27.91 μA). the simultaneously determination of AA, DA and UA detecting, the well three defined positive peak potential and positive current in neutral PBS (pH = 7) electrolyte media. good stable, low detection limit of AA, DA and UA were 3.3, 10 and 13.33×10^{-7} M and limit of quantification were 10, 30, 40×10^{-7} M.

3.6.1.2. Effect of scan rate AA, DA, and UA. The effect of scan rates was evaluated by CVs at CoTGPc/GCE in PBS (pH = 7) electrolyte system containing 10 μM AA and 10 μM DA at the scan rate ranges from 50 to 250 mV s^{-1}, as shown in Fig.8A and 8C. The positive (Ipc) current was increased by increasing the scan rates which indicates the substrate was fully transferred into the CoTGPc/GCE surface. It was attributed to the

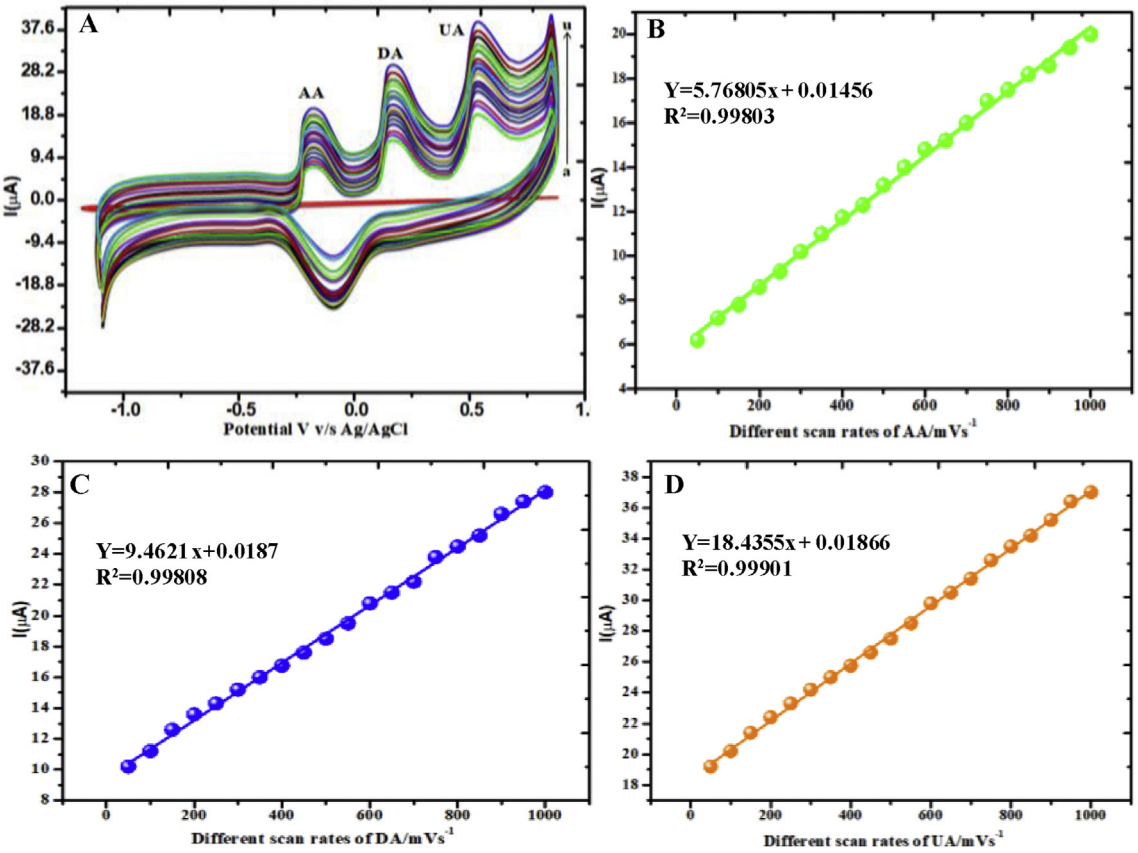

Fig. 9. CV plots recorded of CoTGPc/GCE in PBS (pH=7) electrolyte system peaks at; (A) Different scan rate a-u (50-1000 mVs^{-1}) of AA, DA and UA. Linear plot of cathodic peak current vs. different scan rates of (B) AA, (C) DA and (D) UA/mVs^{-1}.

fast electron transfer process. Fig.8A and 8C inset (upper) shows that the Linear plot of Ipc vs. square roots of the scan rates of AA and DA, both Ip was linearly increased by increasing scan rates, which shows that the oxidation process of AA and DA at tetra ganciclovir CoPc/GCE is diffusion controlled process. Besides, the effect of scan rates on the peak potential of anodic (AA, Epa) and positive (DA, Epc) behavior was also investigated. Fig.8A and 8C inset describes that the linear relationship between the Epa/Epc and logarithm of scan rates and it gives two straight lines. The linear regression equation was obtained for AA, Epa (V) = 1.38 logv+0.06 and DA, Epc (V) = 20.23 logv+0.0484 with a correlation coefficient of 0.99663 and 0.99687, respectively as shown in inset Fig.8B and 8D.

Cyclic voltammetry for AA, DA, and UA was carried out at different scan rates. Results indicated that there is a linear relationship between the peak current (I_p) and the scan rate (v) in the range of 50–1000 mVs^{-1}. Also, there is a linear relationship between the peak current (*I*p) and the square root of the scan rate ($V^{1/2}$) in the scan rates for all species, which indicates that in addition to the existence of a diffusion-controlled mechanism, surface controlled reaction mechanisms are prevailing for electrochemical reactions at slow scan rates. The variation of reaction mechanisms from surface controlled to diffusion controlled at high sweeping rates indicates that faster charge transfer kinetics that could follow higher scan rates of CoTGPc/GCE. With increasing scan rate, the oxidation peak potentials for all three species shift to a positive direction [33]. The electrooxidation processes were explored with the different and same concentration of the biomolecules in simultaneous detection. The result reflects are shown in Fig. 9A. The slope of the linear regression line for each species was nearly equal to slope without the absence of other species of Ipc v/s different scan rates (50-1000 mVs^{-1}), indicating that they do not interfere in the determination. Calibration graph of AA, linear equation is Y = 5.76805 (AA) + 0.01456 and correlation coefficient R^2 = 0.99803 Fig. 9B, for DA linear equation is Y = 9.4621 (DA) + 0.0187 and correlation coefficient R^2 = 0.99808 Fig. 9C and UA linear equation is Y = 18.4355x + 0.01866 and correlation coefficient R^2 = 0.99901 Fig. 9D [10].

3.6.2. Individual determination of AA, DA and UA

3.6.2.1. Detection of AA. Cyclic voltametry experimental plot of CoTGPc/GCE in PBS (pH = 7) electrolyte system, as usual fixed potential (-0.7 to 0.35 V) modified GCE was predicting oxidation anodic peak potential (-0.512 V) as show the substituted CoPc peak. Fig. 10. (Red curve) and 2–10 μM concentration as AA predicting the anodic peak potential (-211 mV) and increasing the concentration by high positive peak current of AA, Fig. 10A. The slope of the linear regression line for the calibration graph of AA species is nearly equal to that without the other species positive peak current vs. different concentration of AA (2–10 μM), indicating that they do not interfere in the determination of each other. Calibration graph of AA are linear equation is Y = 1.735 (AA) + 3.47 and correlation coefficient R^2 = 0.9989 Fig. 10B. At constant of AA predicting the potential and increasing the scan rates (10-100 mVs^{-1}) by highly increasing the positive peak current Fig. 10C. And calibration graph of AA is linear equation is Y = 0.19901 (AA) + 12.72267 and correlation coefficient R^2 = 0.99923 Fig. 10D. The CoTGPc/GCE is AA

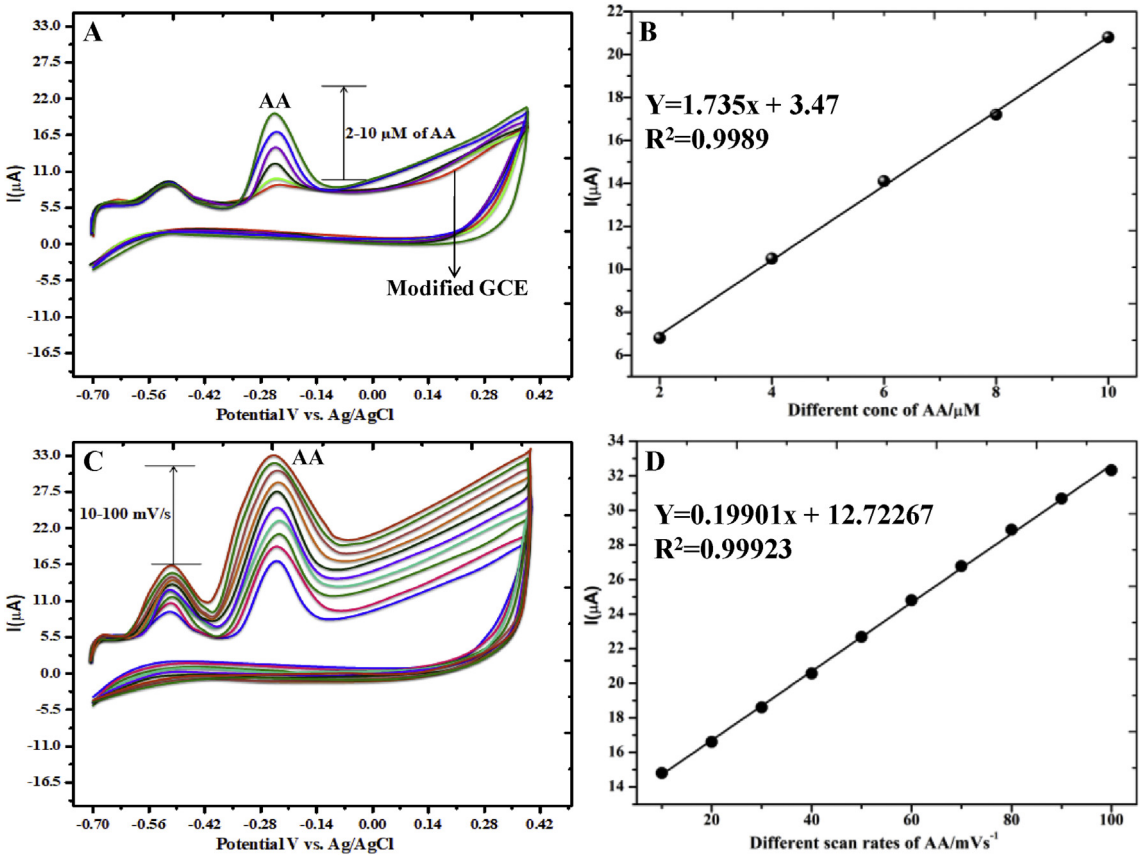

Fig. 10. CVs plot of CoTGPc/GCE in PBS (pH=7) electrolyte system peaks at; (A) Different concentrations 2-10 µM of AA at scan rate 50 mVs^{-1}, (B) Linear plot of peak current vs. different concentrations of AA/µM, (C) Different scan rate (10-100 mV/s) of AA and (D) Linear plot of positive peak current vs. different scan rates of AA.

predicting the anodic peak potential (-211 mV) as compare to shown in Fig. 7 inset c curve.

3.6.2.2. Detection of DA. Cyclic voltametry experimental plot of CoTGPc/GCE in PBS (pH = 7) electrolyte system, as usual fixed potential (-0.7 to 0.35 V) modified GCE was predicting oxidation anodic peak potential (-0.523 V) as show the substituted CoPc peak. Fig. 11A. (inset red curve) and 2–10 µM concentration of DA predicting the positive peak potential (251 mV) and another one reversible peak at positive potential (130 mV), DA is also reversible peak at positive potential, DA predicting the well defined peak potential, and increasing the concentration of DA by increasing high positive current Fig. 11A. The slope of the linear regression line for the calibration graph of DA species is nearly equal to that without the other species of positive current vs. different concentration of DA (2–10 µM), indicating that they do not interfere in the determination of each other. Calibration graph of DA, linear equation is Y = 2.54 (DA) + 3.76 and correlation coefficient R^2 = 0.9995 Fig. 11B. At constant of DA predicting the positive peak potential by increasing the scan rates (10-100 mVs^{-1}), the increases scan rates by increasing high positive current Fig. 11C. And calibration graph of DA, linear equation is Y = 0.3517 (DA) + 9.5667 and correlation coefficient R^2 = 0.99643 Fig. 11D. The CoTGPc/GCE is DA predicting the positive peak potential (251 mV) as compare to shown Fig. 7 inset d curve.

3.6.2.3. Detection of UA. Cyclic voltametry experimental plot of CoTGPc/GCE in PBS (pH = 7) electrolyte system, as usual potential (-0.7–0.9 V) modified GCE was predicting oxidation anodic peak potential (-0.552 V) as show the substituted CoPc peak. Fig. 12A. (Red curve) and 2–10 µM concentration of UA predicting the positive peak potential (619 mV), UA predicting the well defined peak potential, and increasing concentration by increasing high positive current Fig. 12A. The slope of the linear regression line for the calibration graph of UA species is nearly equal to that without the other species of positive peak current vs. different concentration of UA (2–10 µM), indicating that they do not interfere in the determination of each other. Calibration graph of UA, linear equation is Y = 1.55 (UA) + 11.2 and correlation coefficient R^2 = 0.99917 as shown in Fig. 12B. At constant of UA predicting the positive peak potential by increasing the scan rates (10–120 mV s^{-1}), detect the high positive current Fig. 12C. And calibration graph of DA, linear equation is Y = 0.27161 (UA) + 1.81212 and correlation coefficient R^2 = 0.99896 Fig. 12D. The CoTGPc/GCE is UA predicting the positive peak potential (619 mV) as compile same result shown Fig. 7 inset e curve.

3.6.3. DPV studies

3.6.3.1. Differential pulse voltammetric studies of AA, DA, and UA. The DPV was carried out for the mixtures of AA, DA, and UA, in the potential range of −0.8 to +1.0 V in PBS (pH = 7) electrolyte solution (Fig. 13A) and pulse duration: t_{pulse} = 200 ms, pulse height: E_{pulse} = 50 mV, staircase ramp: t_{step} = 500 ms, E_{step} = 5 mV, the result shows a well separated three cathodic peak potentials at -135, 235 and 610 mV corresponding to their oxidation for all the species with modified GCE. Peak separations of 100 and 375 mV between AA–DA, and DA–UA, respectively, prompted us to detect AA, DA and UA mixtures by using DPV [25, 26, 27]. The linearity was observed in the concentration range of 2–12 µM for all the three biomolecules under investigation Fig. 13A. The linear equation of AA: Y = 2.3314 AA) + 0.1805, Y = 3.09455 (DA) + 0.35818, UA Y = 3.372 (UA) + 1.4215 and correlation coefficient of R^2 = 0.99726 Fig.13B, R^2 = 0.99814 Fig.13C and R^2 = 0.99677 Fig. 13D, reflects stability and suitable for biological fluids in neutral media of PBS (pH = 7) electrolyte. This was solely attributed to the mediated oxidation

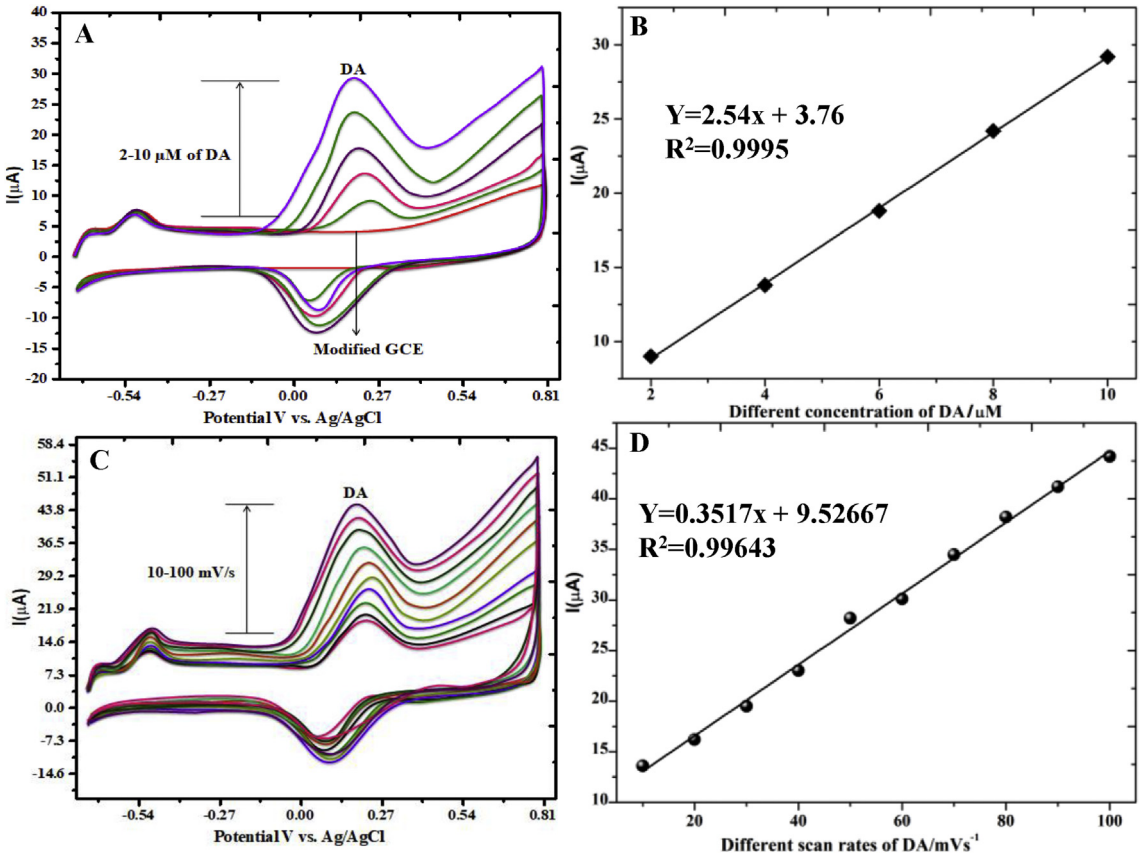

Fig. 11. CVs plot of CoTGPc/GCE in PBS (pH=7) electrolyte system peaks at; (A) Different concentrations 2-10 µM of DA, (B) Linear plot of peak current vs. different concentrations of DA, (C) Different scan rate (10-100 mV/s) of DA and (D) Linear plot of peak current vs. different scan rates of DA.

reaction at modified GCE towards AA, DA and UA mixture Fig. 13.

3.6.3.2. Simultaneously determination of AA, DA, and UA (DPV). A major problem in monitoring AA, DA, and UA using electrochemical technique was the influence of the simultaneous studies. The DPV results show that the modified electrode with CoTGPc has a significant electrocatalytic activity toward the oxidation reactions for all three biomolecules. The DPV curves of modified CoTGPc/GCE in the ternary solutions containing the interfering biomolecules were presented in Fig. 14. The separate peak for 2–12 µM AA was obtained having cathodic peak potential (-131 mV) on CoTGPc/GCE, Fig. 14A. The addition of 2–12 µM DA to the electrolytic cell keeping the AA concentration constant a peak was observed at potential 250 mV Fig. 14C. Further keeping both the concentration of AA and DA constant and continue DPV by adding 2–12 µM UA shows a peak at cathodic potential 610 mV Fig. 14E and the results were in good agreement with potential in CV studies. The DPV studies with CoTGPc/GCE presents good linear responses to the concentration were presented in Fig.144A, C and E. The linear plot of peak current vs different concentrations of AA, DA and UA in µM, linear concentrations plot of Y = 2.88 (AA) + 4.199, Y = 2.91 (DA) + 4.20891 and Y = 2.99 (UA) + 4.26327 with correlation coefficient $R^2 = 0.99851$, 0.99941 and 0.99955 (Fig.14B, D, F). It was concluded that CoTGPc/GCE shows excellent electrochemical sensing activity toward the simultaneous determination of three biomolecules in a ternary solution. This further confirms that CoTGPc/GCE holds a high sensitivity toward the selective electrocatalysis for three biomolecules. Further, it was interesting to note that the sensitivities of the modified GC electrode toward AA, DA, and UA are approximately the same with the sole existence of UA (Fig. 14E), which indicates the facts that the linear range and sensitive determination of DA, AA, and UA were feasible at CoTGPc/GCE. The results were presented in [34] Table 2.

3.6.4. Amperometric sensing of AA, DA, and UA

3.6.4.1. Individual and interference determination of AA, DA, and UA. The high electrocatalytic activity of CoTGPc GCE towards AA, DA and UA makes it attractive for the construction of nonenzymatic biosensors for the detection of the biomolecules. Fig. 15 depicts the amperometric individual responses of CoTGPc/GCE on the successive addition of a series of concentrations of AA, DA, and UA. The modified GCE responds quickly and sensitively with an evident current signal to each addition of 10 µM of AA at the fixed potential of -0.200 V. Addition of different amounts of AA (5–45 µL) as shown in Fig. 15A. 15 µM DA at a fixed potential of +0.400 V, predict the same positive current increase, and the response reaches the maximum steady-state current within 50 Sec. Fig. 15C. Illustrates typical amperometric responses for the successive addition of a 20 µM of UA at fixed potential +0.600 V. Intense current response can be clearly observed for each addition of UA within a normal period of time 50s Fig. 15E. The calibration curves indicates that the modified CoTGPc/GCE-based biosensor has good linear responses to, AA, DA, and UA concentrations for the different amounts ranges from 5-45 µL, linear plot of Ipc V/S different amounts of AA, DA and UA satisfies the linear equations: Y = 0.482 (AA) – 0.289, Y = 0.812 (DA) – 0.306, and Y = 0.856 (UA) – 0.961, with correlation coefficient of $R^2 = 0.9998$, $R^2 = 0.9996$, $R^2 = 0.9975$ (Fig.15B, D, F). CoTGPc/GCE shows great application potential to construct nonenzymatic biosensor towards three biomolecule detection with rapid response, high sensitivity and good reproducibility [34, 35, 36] (Fig. 16A). shows the amperometric curve obtained for the interference addition of (2, 5, 10 µM) AA, DA and UA at CoTGPc/GC electrode in a homogeneously stirred PBS (pH = 7) electrolyte system at an applied potential of +0.600 V and the current response was highly increased. Moreover, a steady state current response was attained within the 50s after the interference of each

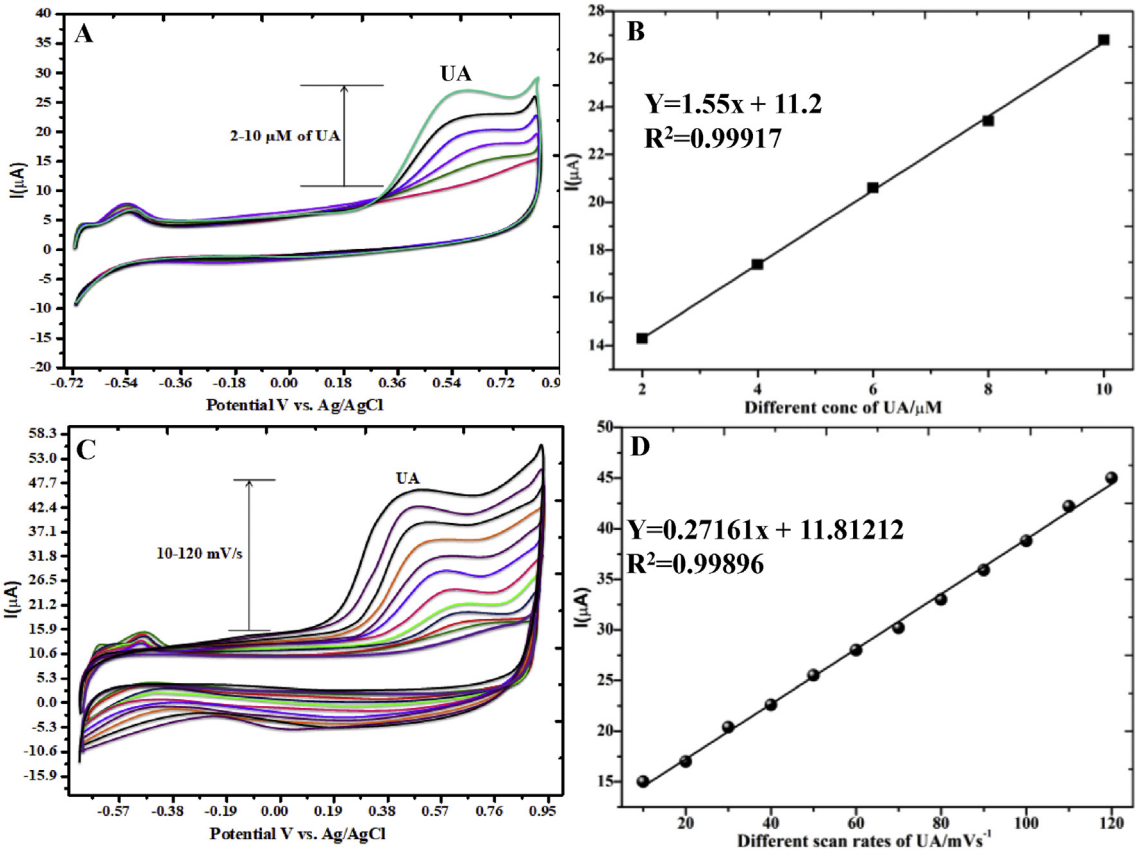

Fig. 12. CVs plot of CoTGPc/GCE in PBS (pH=7) electrolyte system peaks at; (A) Different concentrations 2-10 μM of UA, (B) Linear plot of peak current vs. different concentrations of UA, (C) Different scan rate (10-120 mV/s) of UA and (D) Linear plot was positive peak current vs. different scan rates of UA.

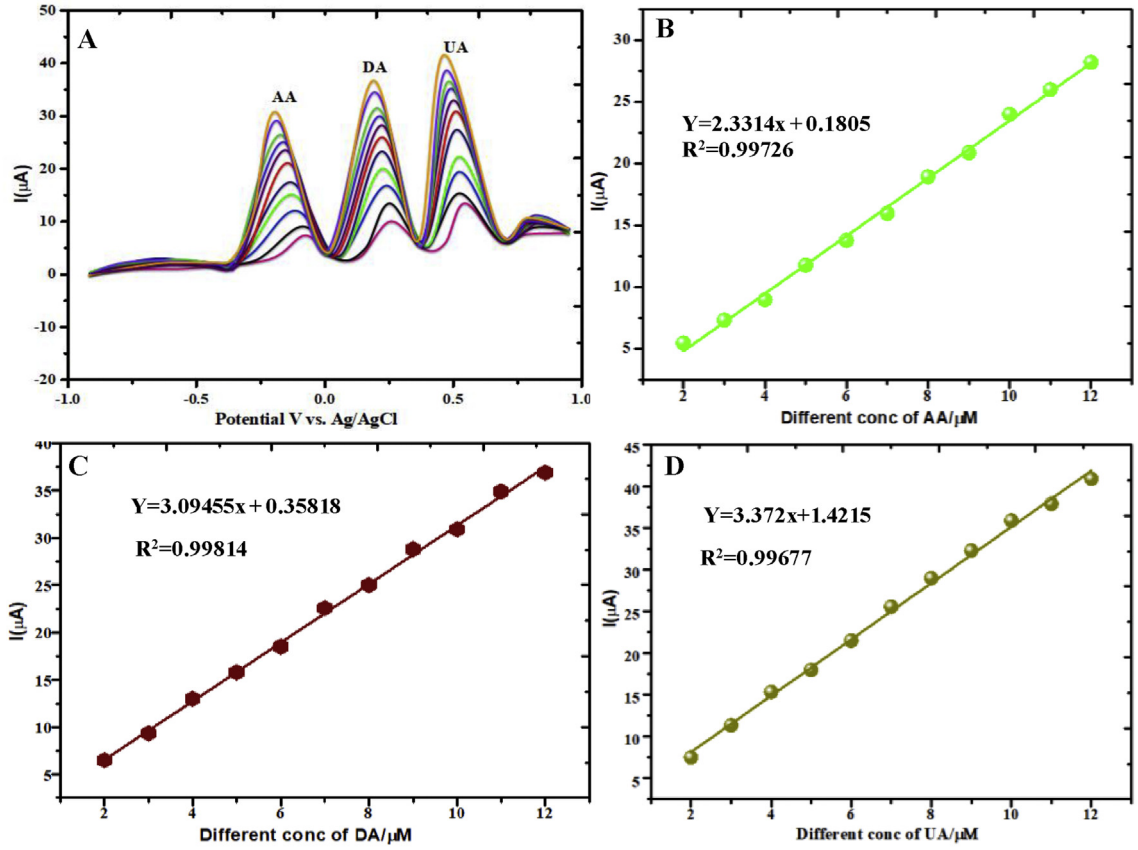

Fig. 13. DPV plots recorded of CoTGPc/GCE in PBS (pH=7) electrolyte system peaks at; (A) Mixtures determination of 2–12×10^{-6} M of AA, DA and UA. Linear plot of Ipc vs. different concentrations of (B) AA, (C) DA and (D) UA/μM. at scan rate= 50 mV/s.

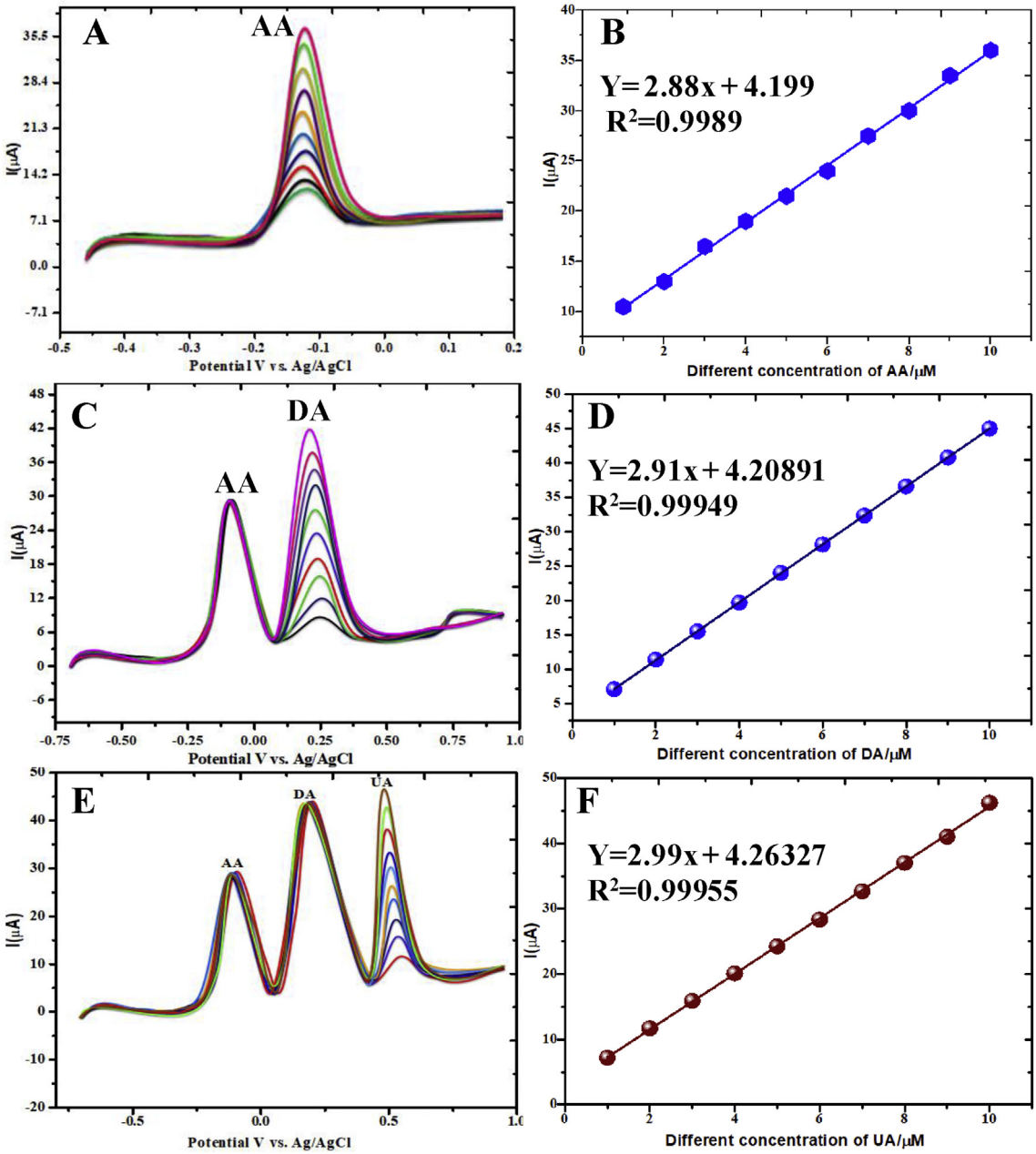

Fig. 14. DPV plots recorded of CoTGPc/GCE in PBS (pH=7) electrolyte system peaks at; simultaneously determination of 2–12×10^{-6} M, of (A) AA, (C) DA and (E) UA. Linear plot of Ipc vs. different concentration of (B) AA, (D) DA and (F) UA/μM. at scan rate= 50 mV/s.

analyte. A systematic increase in current response was observed for the interference addition of AA, DA, and UA. We have estimated the current response for interference addition of AA, DA, and UA from (Fig. 16A). Linear plot of Ipc V/S different concentrations of AA, DA and UA/μM satisfies the linearity: linear equation; Y = 8.70739x – 14.26667, and correlation coefficient of R^2 = 0.98798 (Fig. 16B). The modified CoTGPc/GCE exhibits good responses towards detection of the cathodic peak current [4, 37].

3.6.5. *Selectivity studies*

Amperometry interference response at CoTGPC/GCE in (PBS) pH = 7 electrolyte system at successive addition of different analytes for (10×10^{-6} M) Nitrite (NO_2^-), Hydrogen Peroxide (H_2O_2) and Glucose (GOx) are detections with negligible currents responses by during AA, UA and DA; at applied potential for +0.600 V (Fig. 17), this results indicates that good selectivity of modified CoTGPc/GC electrode.

3.6.6. *Determination of real sample analysis*

3.6.6.1. Ascorbic acid in vitamin C tablets. Vitamins 'C' tablet, containing 200 mg $tablet^{-1}$ AA, was finely powdered, and approximately equivalent to 200 mg of vitamin C to 100 mL of water, shaken for 20 min and filtered into a 100 mL volumetric flask. The residue was washed several times with water and the solution was diluted to the mark. 10 μL of the sample was diluted to 10 mL with PBS (pH 7) and then transferred to an electrolytic cell for the determination of AA by CoTGPc/GCE. The vitamin C tablets of AA were analyzed by the standard addition method. The results are in Table 3.

3.6.6.2. Dopamine in dopamine hydrochloride injections. In order to verify the reliability of the method for analysis of DA in pharmaceutical

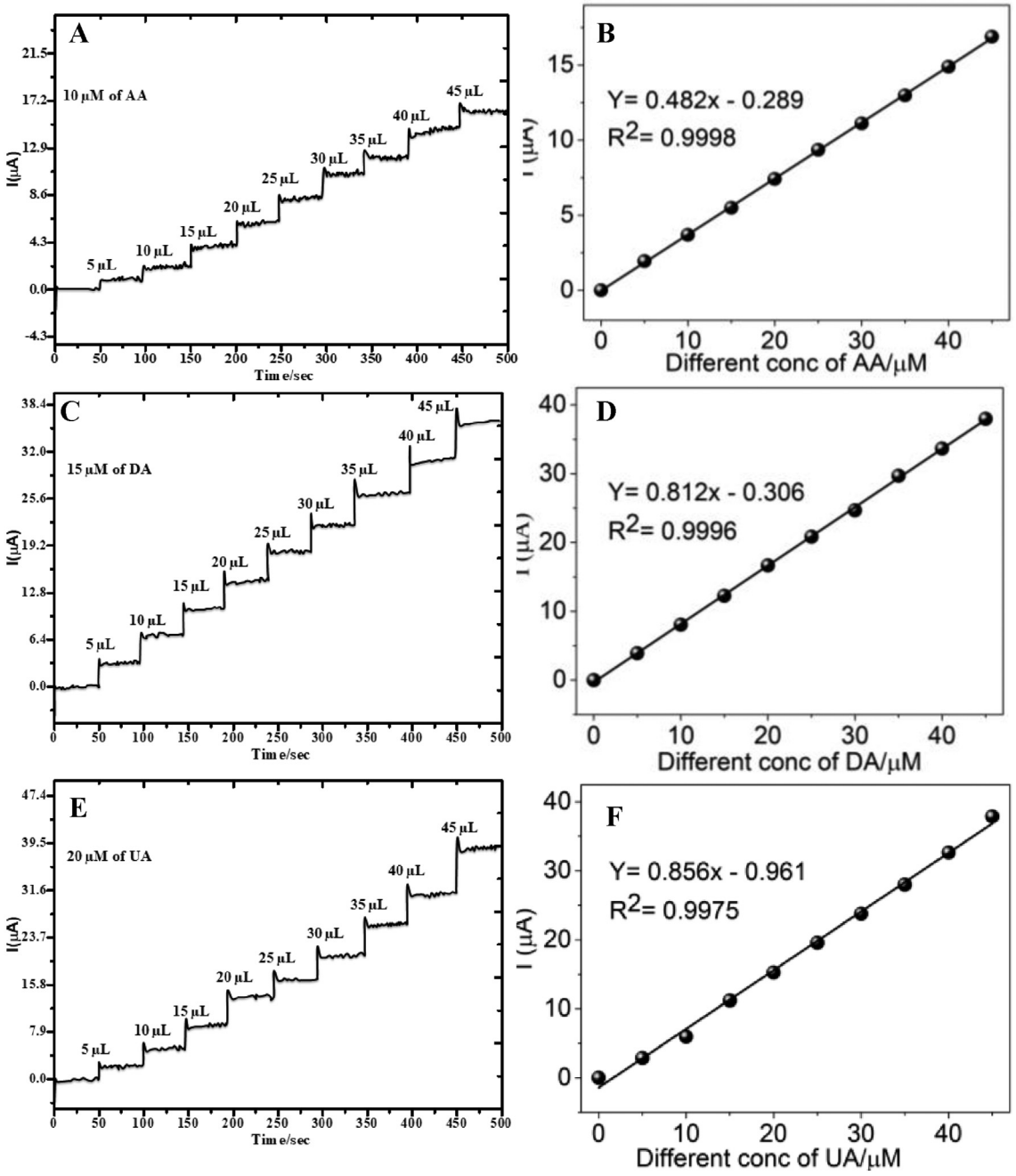

Fig. 15. Amperometric individual response of CoTGPc/GCE in PBS (pH=7) electrolyte system peaks at; (A), (C), (E) various amounts (5-45 μL) of 10, 15, 20 μM for AA, DA UA; at fixed potential were -0.200 +0.400 and +0.700 V, and Linear plot of cathodic peak current (*I*pc) vs. different amounts of (B) AA, (D) DA and (E) UA.

product, 20 μL of the dopamine hydrochloride injection solution was injected into a 10mL volumetric flask and made up to volume with PBS (pH 7). Then this test solution was placed in an electrochemical cell for the determination of DA using the CV method. The analytical results are listed in Table 3. The results were satisfactory, showing that the proposed methods could be efficiently used for the determination of DA in injections.

3.6.6.3. Uric acid in a human urine sample. The utilization of the proposed method in real sample analysis was also investigated by direct analysis of UA in the human urine sample. One person 30 μM and second person 40 μM urine samples used for detection were diluted 2 times with PBS (pH 7). The results are listed in Table 3. The recovery of the spiked samples 96.7 and 101.2%, indicating the detection procedures are free from interferences of the urine sample matrix.

4. Conclusion

In conclusion, a new CoTGPc macromolecule was synthesized and characterized by FT-IR, UV-Vis, MASS spectra and elemental analysis, electronic spectroscopy XRD and TGA. The obtained compounds show maximum visible light absorption from 200-700 nm and exhibit improved thermal stability and solubility in common organic solvents such as concentrated sulfuric acid, N, N-dimethylformamide, and dimethylsulfoxide. A simple and green electrochemical method was utilized to fabricated to CoTGPc/GCE for simultaneous determination of AA, DA,

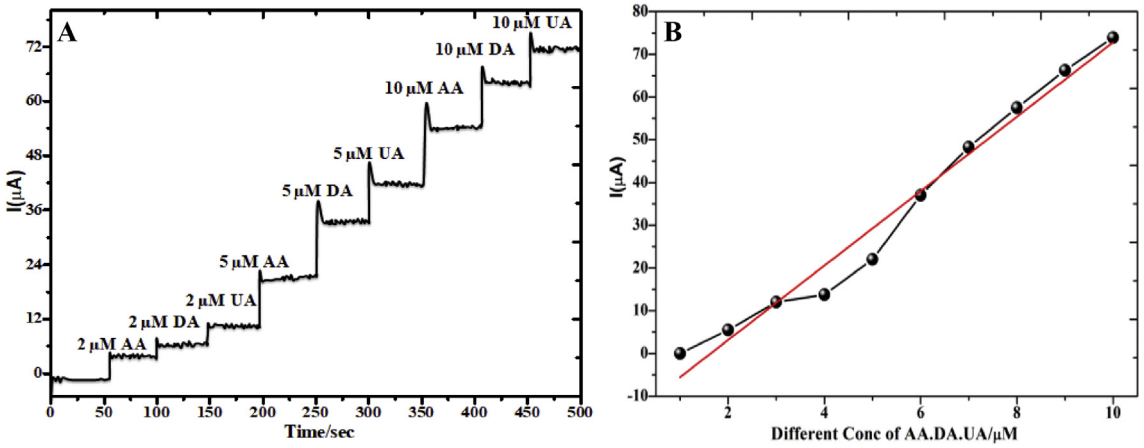

Fig. 16. Amperometric response of CoTGPc/GCE in (PBS) pH=7 in electrolyte system peaks at; (A) interference addition of different concentration (2, 5 and 10×10^{-6} M) AA, DA and UA, (B) Linear plot of peak current vs. different concentrations of AA, DA and UA; at fixed potential +0.700 V.

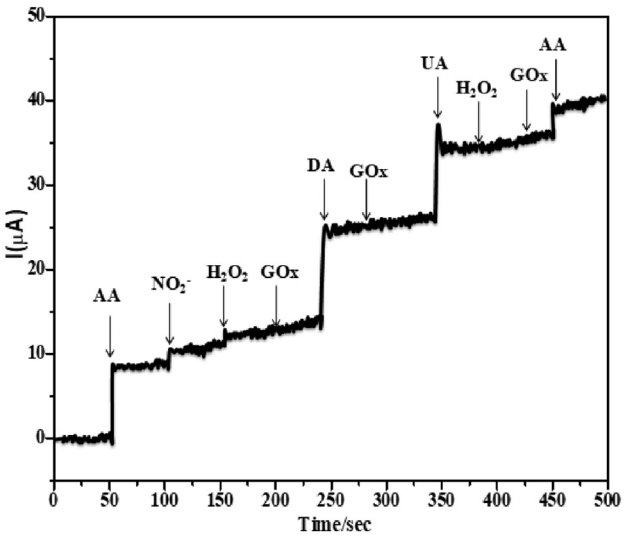

Fig.17. Selectivity studies of interfering species like Nitrite (NO_2^-), Hydrogen Peroxide (H_2O_2) and Glucose (GOx) by during AA, DA and UA.

Table 3
Analytical data for the commercial AA in Vitamin 'C' tablet, DA in dopamine hydrochloride injection and UA in human urine samples.

samples	Theoretical valve	Detected	Spiking	Recovery (%)	RSD[g] (%)
Vitamin 'C' tablets	10 µM	10.2 µM	10 µM	102 %	0.28
Dopamine Hydrochloride Injection	20 µM	21.5 µM	20 µM	107.5 %	0.34
Urine Sample	30 µM	29 µM	30 µM	96.7 %	0.43
	40 µM	40.5 µM	30 µM	101.2 %	

g = average of three replicate analysis.

and UA by cyclic voltammetry (CV), different pulse voltammetry (DPV) and chronoamperometry (CA) techniques. High selectivity was achieved by the CoTGPc/GC modified electrode for all the three biomolecules under investigation with good sensitivity, linear responses, reproducibility, and low detection limit. The results of this work indicate that the high electrocatalytic active in nature. And determinations of real samples analysis were AA in vitamin "C" tablet, DA in dopamine hydrochloride injections and Human urine in UA.

Declarations

Author contribution statement

K. R. V. Reddy: Conceived and designed the experiments.
Mounesh: Performed the experiments; Wrote the paper.
C. D. Mruthyunjayachari, N. Y. P. Kumara: Analyzed and interpreted the data.
P. Malathesh, B. S. Jilani: Contributed reagents, materials, analysis tools or data.

Funding statement

This research did not receive any specific grant from funding agencies in the public, commercial, or not-for-profit sectors.

Competing interest statement

The authors declare no conflict of interest.

Additional information

No additional information is available for this paper.

References

[1] M.L.A.V. Heien, A.S. Khan, J.L. Ariansen, J.F. Cheer, P.E.M. Phillips, R.M. Wightman, Real-time measurement of dopamine fluctuations after cocaine in the brain of behaving rats, in: Proceedings of the National Academy of Sciences of theUnited States of America, 102, 2005, pp. 10023–10028.
[2] Mounesh, B.S. Jilani, P. Malatesh, K.R. Venugopala Reddy, K.S. Lokesh, Simultaneous and sensitive detection of ascorbic acid in presence of dopamine using MWCNTs-decorated cobalt (II) phthalocyanine modified GCE, Microchem. J. 147 (2019) 755–763.
[3] O. Arrigoni, M.C.D. Tullio, Ascorbic acid: much more than just an antioxidant, Biochim. Biophys. Acta 1569 (2002) 1–9.
[4] P. Kalimuthu, S.A. John, Electropolymerized film of functionalized thiadiazoleon glassy carbon electrode for the simultaneous determination of ascorbic acid, dopamine and uric acid, Bioelectrochem. 77 (2009) 13–18.
[5] J.H. Kim, J.M. Auerbach, J.A.R. Gómez, I. Velasco, D. Gavin, N. Lumelsky, S.H. Lee, J. Nguyen, R.S. Pernaute, K. Bankiewicz, R. McKay, Dopamine neurons derived from embryonic stem cells function in an animal model of Parkinson's disease, Nature 418 (2002) 50–56.
[6] S. Corona-Avendaño, G. Alarcón-Angeles, M.T. Ramírez-Silva, G. Rosquete-Pina, M. Romero-Romo, M. Palomar-Pardavé, On the electrochemistry of dopamine in aqueous solution. Part I: the role of [SDS] on the voltammetric behavior of dopamine on a carbon paste electrode, J. Electroanal. Chem. 609 (2007) 17.
[7] M. Palomar-Pardavé, G. Alarcón-Ángeles, S. Corona Avendaño, M. Romero-Romo, A. Merkoçi, A. Rojas-Hernández, M.T. Ramírez-Silva, Electrochemical study of the formation of surface inclusion complex of ascorbic acid with immobilized

β-ciclodextrin and carbon nanotubes over a carbon paste electrode, Electrochem. Soc. Trans. 36 (2011) 431–438.

[8] K.C.F. Toledo, B.M. Pires, J.A. Bonacin, B.A. Iglesias, Stabilization of meso-tetraferrocenyl-porphyrin films by formation of composite with Prussian blue, J. Porphyr. Phthalocyanines 21 (2017) 10–15.

[9] Y. Wang, Y. Li, L. Tang, J. Lu, Application of graphene-modified electrode for selective detection of dopamine, Electrochem. Commun. 11 (2009) 889–892.

[10] Lu Yang, Dong Liu, Jianshe Huang, Tianyan You, Simultaneous determination of dopamine, ascorbic acid and uric acidat electrochemically reduced graphene oxide modified electrode, Sensor. Actuator. B 193 (2014) 166–172.

[11] J.H. Zagal, S. Griveau, J. Silva, T. Nyokong, F. Bedioui, Metallophthalocyanine-based molecular materials as catalysts for electrochemical reactions, Coord. Chem. Rev. 254 (2010) 2755–2791.

[12] V. Mani, R. Devasenathipathy, S.-M. Chen, J.-A. Gu, S.-T. Huang, Synthesis and characterization of graphene-cobalt phthalocyanines and graphene-iron phthalocyanine composites and their enzymatic fuel cell application, Renew. Energy 74 (2015) 867–874.

[13] K. Wang, J.-J. Xu, H.-Y. Chen, A novel glucose biosensor based on the nanoscaled cobalt phthalocyanine–glucose oxidase biocomposite, Biosens. Bioelectron. 20 (2005) 1388–1396.

[14] K.M. Pradeep, K.R. Venugopala Reddy, M.N. K Harish, B. Chidananda, B.J. Madhu, C.D. Mruthyunjayachari, S.D. Ganesh, Poly(1,3,4-oxadiazole-aryl ether) embedded metalphthalocyanines: synthesis, characterization and electrical studies, J Synthetic metal 185–6 (2013) 79–88.

[15] G.P. Shaposhnikov, V.E. Maizlish, V.P. Kulinich, Carboxy-substituted phthalocyanine metal complexes, Russ. J. Gen. Chem. 75 (2005) 1480–1488.

[16] X. Sun, L. Wang, Z. Tan, Improved synthesis of metal-free/Metal phthalocyanine Tetracrboxylic acids and their applications in the catalytic epoxdiation of cyclohexene, Catal. Lett. 145 (2015) 1094–1102.

[17] B. Chidananda, K.R. Venugopala Reddy, K.M. Pradeep, M.N.K. Harish, C.D. Mruthyunjayachari, S.D. Ganesh, N.S. Vijaykumar, P. Malthesh, 2, 9, 16, 23-tetra-N-(4-bromo-2-methoxyphenyl)benzamide substituted metallophthalocyanines: synthesis, characterization, antimicrobial and antioxidant activity, Der Pharma Chem. 8 (10) (2016) 198–204.

[18] B. Chidananda, K.R. Venugopala Reddy, M.N.K. Harish, K.M. Pradeep, C.D. Mruthyunjayachari, S.D. Ganesh, Synthesis, characterization, novel interaction of DNA, Antioxidant and Antimicrobial studies of new water soluble metallophthalocyanines posture eight hydroxyphenyl moiety via 1,3,4-oxadiazole bridge, J heterocyclic chem 52 (2014) 1782–17913.

[19] N. Manjunatha, M. Imadadulla, K.S. lokesh, K.R. Venugopala Reddy, Synthesis and electropolymerization of tetra-[β-(2-benzimidazole)] and tetra-[β-(2-(1-4(-aminophenyl)) benzimidazole)] embedded cobalt phthalocyanine and their supercapacitance behaviour, Dyes Pigments 153 (2008) 213–224.

[20] M. Imdadulla, N. Manjunath, K.S. Lokesh, Solvent dependent dispersion behavior of mcrocylce stabilized cobalt nanoparticles and their applications, New J. Chem. 42 (2018) 11363–11372.

[21] K.S. Lokesh, Layer-by –layer self assembly of a water soluble phthalocyanine on gold. Application to the electrochemical determination of hydrogen peroxide, Bioelectrochemistry 91 (2013) 21027.

[22] J.P. Fan, X.M. Zhang, M. Ying, Electrocatalytic activity of electropolymerized cobalt tetraaminophthalocyanine film modified electrode towards 6-mercaptopurine and 2-mercaptobenzimidazole, S. Afr. J. Chem. 63 (2010) 145–151.

[23] A.A. Ebert Jr., H.B. Gottlieb, Infrared spectra of organic compounds exhibiting polymorphism, J. Am. Chem. Soc. 74 (11) (1952) 2806–2810.

[24] K. S Lokesh, A. Adriaens, Synthesis and characterization of tetra-substituted palladium phthalocyanine complexes, Dyes Pigments 96 (1) (2013) 269–277.

[25] S. Thiagarajan, S.-M. Chen, Preparation and characterization of PtAu hybrid film modified electrodes and their use in simultaneous determination of dopamine, ascorbic acid and uric acid, Talanta 74 (2007) 212–222.

[26] A.I. Gopalan, K.P. Lee, K.M. Manesh, P. Santhosh, J.H. Kim, J.S. Kang, Electrochemical determination of dopamine and ascorbic acid at a novel gold nanoparticles distributed poly(4-aminothiophenol) modified electrode, Talanta 71 (4) (2007) 1774–1781.

[27] Afsaneh Safavi, Norouz Maleki, Omran Moradlou, Fariba Tajabadi, Simultaneous determination of dopamine, ascorbic acid, and uric acid using carbon ionic liquid electrode, J. Anal. Biochem. 359 (2006) 224–229.

[28] J. Oni, T. Nyokong, Simultaneous voltammetric determination of dopamine and serotonin on carbon paste electrodes modified with iron(II) phthalocyanine complexes, Anal. Chim. Acta 434 (2001) 9.

[29] S. Yuan, W. Chen, S. Hu, Fabrication of TiO_2 nanoparticles/surfactant polymer complex film on glassy carbon electrode and its application to sensing trace dopamine, Mater. Sci. Eng. 25 (2005) 479–485.

[30] E.B. Bustos, Ma.G.G. Jimenez, B.R.D. Sanchez, E. Juaristi, T.W. Chapman, L.A. Godnez, Glassy carbon electrodes modified with composites of starburst-PAMAM dendrimers containing metal nanoparticles for amperometric detection of dopamine in urine, Talanta 72 (2007) 1586–1592.

[31] F.C. Moraes, M.F. Cabral, Sergio A.S. Machado, Lucia H. Mascaro, Electrocatalytic behavior of glassy carbon electrodes modified with multiwalled carbon nanotubes and cobalt phthalocyanine for selective analysis of dopamine in presence of ascorbic acid, Electroanalysis 20 (2008) 851–857.

[32] A.A. Ensafi, M. Taei, T. Khayamian, A. Arabzadeh, Highly selective determination of ascorbic acid, dopamine, and uric acid by differential pulse voltammetry using poly (sulfonazo III) modified glassy carbon electrode, Sensor. Actuator. B 147 (2010) 213–221.

[33] C. Karuppiah, R. Devasenathipathy, S.M. Chen, D. Arulraj, S. Palanisamy, V. Mani, V.S. Vasantha, Fabrication of nickel tetrasulfonated phthalocyanine functionalized multiwalled carbon nanotubes on activated glassy carbon electrode for the detection of dopamine, Electroanalysis 27 (2015) 485–493.

[34] J. Hou, C. Xu, D. Zhao, J. Zhou, Facile fabrication of hierarchical nanoporous AuAg alloy and its highly sensitive detection towards dopamine and uric acid, J. Sensors Actuators B 225 (2016) 241–248.

[35] M. Noroozifar, M. Khorasani-Motlagh, R. Akbari, M. Bemanadi Parizi, Simultaneous and sensitive determination of a quaternary mixture of AA, DA, UA and Trp using a modified GCE by iron ion-doped natrolite zeolite-multiwall carbon nanotube, Biosens. Bioelectron. 28 (2011) 56–63.

[36] H. Yao, Y. Sun, X. Lin, Y. Tang, L. Huang, Electrochemical characterization of poly (eriochrome black T) modified glassy carbon electrode and its application to simultaneous determination of dopamine, ascorbic acid and uric acid, J. Electrochim. Acta. 52 (2007) 6165–6171.

[37] H.S. Wang, T.H. Li, W.L. Jia, H.Y. Xu, Highly selective and sensitive determination of dopamine using a Nafion/carbon nanotubes coated poly (3-methylthiophene) modified electrode, J. Biosens. Bioelectron. 22 (2006) 664–669.

[38] S. Yan, Xi Li, Yan Xiong, M. Wang, L. Yang, X. Liu, X. Li, L.A.M. Alshahrani, P. Liu, C. Zhang, Simultaneous determination of ascorbic acid, dopamine and uric acid using a glassy carbon electrode modified with the nickel (II)-bis(1,10-phenanthroline) complex and single-walled carbon nanotubes, J. Microchim. Acta. 183 (2016) 1401–1408.